

NUMERICAL COMPUTATIONS OF CONDUCTIVITIES OVER AGGLOMERATED CONTINUUM PERCOLATION MODELS

Shigeki Matsutani

*Analysis technology center, Canon Inc.
3-3-20, Shimomaruko, Ota-ku, Tokyo 146-8501, Japan
matsutani.shigeki@canon.co.jp*

Yoshiyuki Shimosako

*Analysis technology center, Canon Inc.
3-3-20, Shimomaruko, Ota-ku, Tokyo 146-8501, Japan
shimosako.yoshiyuki@canon.co.jp*

Yunhong Wang

*Analysis technology center, Canon Inc.
3-3-20, Shimomaruko, Ota-ku, Tokyo 146-8501, Japan **

Received Day Month Year

Revised Day Month Year

We numerically investigate the conductivities of continuum percolation models consisting of overlapped particles using the finite difference method as a sequel of our previous article (Int. J. Mod. Phys. **21** (2010), 709). As the previous article showed the shape effect of each particle by handling different aspect ratios of spheroids, in this article we numerically reveal influences of the agglomeration of the particles on conductivities. We conclude that the agglomeration effect on the conductivities can be interpreted as the size effect of an analyzed region.

Keywords: continuum percolation; conductivity; critical exponents; agglomerated particles

PACS Nos.: 05.10.-a, 05.10.Ln, 05.60.Cd, 64.60.ah, 72.80.Ng, 73.22.-f

1. Introduction

As in the previous article,¹ we investigate conductivities of a percolation model using the finite difference method (FDM).² The purpose of this article and the previous one is to clarify how the percolation theory governs the conductivities in real materials which consist of small conductive particles, *e.g.*, nanoparticles, with random configurations. In general, the small particles in a real material have some typical sizes, shapes like spheroids, and cluster structures due to their agglomeration.³⁻⁸

*Present address: Microcreate System Co., 2-1-15 4C, Chuou Yamato Kanagawa 242-0021 Japan.

The purpose of this article is to investigate an agglomeration effect on the conductivity whereas the previous one is on the effect of the shape of each particle. We propose a simple numerical algorithm to simulate an agglomerated configuration of particles though there are some physical models which numerically simulate the agglomerated phenomena.^{9,10} In this article, we employ the simple algorithm. Since our algorithm has a parameter which controls the agglomerated configurations consistently without any difficulties, we numerically show how the conductivity depends upon the agglomerations. Then we also show that one of the agglomeration effects on the conductivity can be interpreted as the size effect of the system by means of numerical computations.

The conductivity is one of the most concerned phenomena in the percolation theory^{11–16} and it is important to investigate the conductivity curve

$$\sigma_{\text{total}} = c(p - p_c)^t, \quad (1)$$

where c is a constant factor, p is the volume fraction, p_c is the percolation threshold, and t is the critical exponent of the conductivity. The behaviors of the threshold p_c and the exponent t represent the conductive properties of the systems in the percolation phenomena, which have some universal properties. It means that their dependence on some parameters of a model is sufficiently weak due to the randomness. In order to discuss the universality, the percolation theory is, ordinarily, based upon a system with the infinite size.^{11–18}

However when we apply the percolation theory to the real composite materials of conductive nanoparticles, we encounter effects coming from the shape of the nanoparticles and several characteristics lengths. Besides lattice percolation models which are given on discrete lattices, the continuum percolation model (CPM) was introduced as in Refs. 11 and 17. In order to handle the size and the shape of particles, CPM has been studied. In the previous article,¹ we studied the shape effects on the conductivities in CPMs among the different aspect ratios of spheroids, where we allowed overlap of the particles. The previous article shows that the conductivity in CPM strongly depends upon the shape of the composed particles.

In this article, we will consider another shape effect or the agglomerated effect of these stuffed spherical particles on the conductivity. With the development of the technology, smaller size of the particles within smaller size of the devices has been produced. When we investigate the conductivities in the real composite materials of conductive nanoparticles from the viewpoint of the percolation theory, we handle three characteristic lengths, i.e., 1) the size of the particle as a minimal size, 2) the size of the system, e.g., the thickness of the film, as the maximal size, and 3) the size of the percolation cluster which is given by a multiplication of the size of the particles and is also related to the size of the system. When the size of devices is sufficiently small, it is important to consider the size effect of the system though the conductivities in the system with infinite size are basically concerned in the percolation theory. In other words, in order to apply the percolation theory to a real material system, it is crucial to consider the relations among the scales.

When the size of particles is smaller such as nanometer scale, due to their interface energy, the particles are basically agglomerated more as a physical phenomenon. Agglomeration forms agglomerated clusters and the cluster brings the the fourth characteristic scale to the system. Thus the evaluation of the agglomeration effect on the conductivity is very important. By employing the simple algorithm to simulate the agglomeration of particles, we numerically give a series of agglomerated configurations of CPM, which we call *agglomerated continuum percolation models* (ACPMs), and investigate the conductive properties of ACPMs by means of FDM. In this article, we also handle the overlapping particles.¹ We show the dependence of the conductivity curves on the agglomeration as in Figure 7.

Since the finite size effects in the conductivity on a percolation model were studied in Chap. 4 of Ref. 11, based upon these studies, we numerically consider the relation between the size effects and the properties in the conductivities in ACPMs. As a result, we show that one of the agglomerated effects on the conductivities with ACPM can be regarded as the size effects of the system.

Conversely it implies that the agglomeration would not have the effect on the universality class of the conductivity curve (1), and thus we numerically show that for an agglomerated configuration, if we properly deal with a system with sufficiently large size, the conductivity might behaves as the uniform random one.

Contents in this article are as follows. §2 shows our computational method. §2.1 describes our algorithm to construct the agglomerated particles in CPM and the geometrical setting in ACPMs. §2.2 provides the computational method of the conductivity over ACPMs using FDM, which is basically the same as that in the previous article.¹ §3 shows our computational results of the conductivity in ACPMs with the agglomerated particles. In §4, we discuss our results from physical viewpoints. In §5, we summarize the results and the discussions.

2. Geometrical setting of ACPM

In this section, we show our geometrical setting of the ACPM. We model the agglomerated particles out of a simple algorithm which is governed by a parameter $\gamma_{\text{agg}} \in [0, 1]$. We also briefly show the computational method of the conductivities over ACPMs using FDM in §2.2, whose details are described in the previous article.¹

2.1. Agglomeration algorithm

We set particles parameterized by their positions (x, y, z) into a box-region $\mathcal{B} := [0, x_0] \times [0, y_0] \times [0, z_0]$ at random and get a configuration \mathfrak{R}_n as one of CPMs. In this article, we set $x_0 = y_0 = z_0 = L$. The particle corresponds to a stuffed sphere or ball with the same radius ρ , $B_{x_i, y_i, z_i} := \{(x, y, z) \in \mathcal{B} \mid |(x, y, z) - (x_i, y_i, z_i)| \leq \rho\}$. The configuration \mathfrak{R}_n is given by $\mathfrak{R}_n := \bigcup_{i=1}^n B_{x_i, y_i, z_i}$.

By fixing the radius ρ of the particle, $\rho = 1$, and a number $\gamma_{\text{agg}} \in [0, 1]$ which

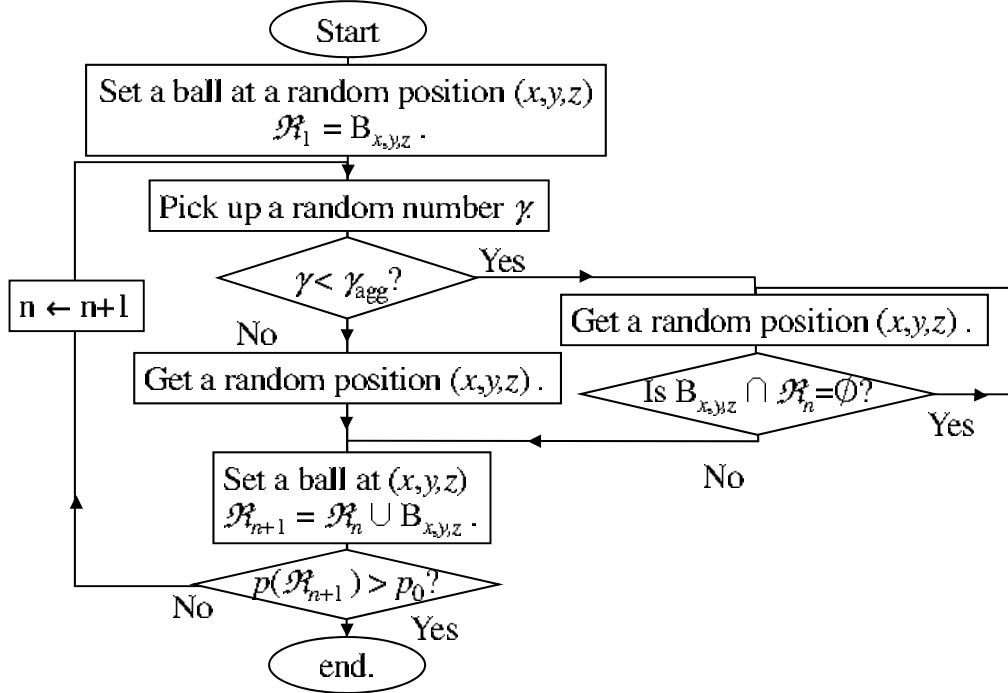
4 *S. Matsutani, Y. Shimosako, Y. Wang*

Fig. 1. The flow chart of the agglomeration configuration algorithm.

is called agglomeration parameter, we introduce an algorithm to construct the configuration \mathfrak{R}_n in ACPM.

We illustrate our algorithm by a flow chart in Figure 1. As an initial state, the configuration \mathfrak{R}_0 has no particle. As the first step, for a uniform random position $(x, y, z) \in \mathcal{B}$ we set a particle $B_{x,y,z}$ whose center is (x, y, z) and the radius is ρ , i.e., $\mathfrak{R}_1 := B_{x,y,z}$.

Let us consider n -step. We take a position (x, y, z) at uniform random in \mathcal{B} , and another random parameter γ at uniform random in $[0, 1]$. If the random parameter γ is greater than γ_{agg} , we employ the position (x, y, z) as the center of a particle and $\mathfrak{R}_{n+1} := \mathfrak{R}_n \cup B_{x,y,z}$. It is noted that we allow the particles to overlap each other.

When the random parameter γ is given as $\gamma \leq \gamma_{\text{agg}}$, we first check whether the ball whose center is the position (x, y, z) is connected with the previous configuration \mathfrak{R}_n or not. If it is connected with the configuration \mathfrak{R}_n , or $\mathfrak{R}_n \cap B_{x,y,z} \neq \emptyset$, we employ the position and add the particle into the configuration \mathfrak{R}_n , or $\mathfrak{R}_{n+1} := \mathfrak{R}_n \cup B_{x,y,z}$.

If not or $\mathfrak{R}_n \cap B_{x,y,z} = \emptyset$, we abandon the position and go on to take another uniformly random position (x, y, z) in \mathcal{B} until we find the position which supplies a connected particle $B_{x,y,z}$ with \mathfrak{R}_n .

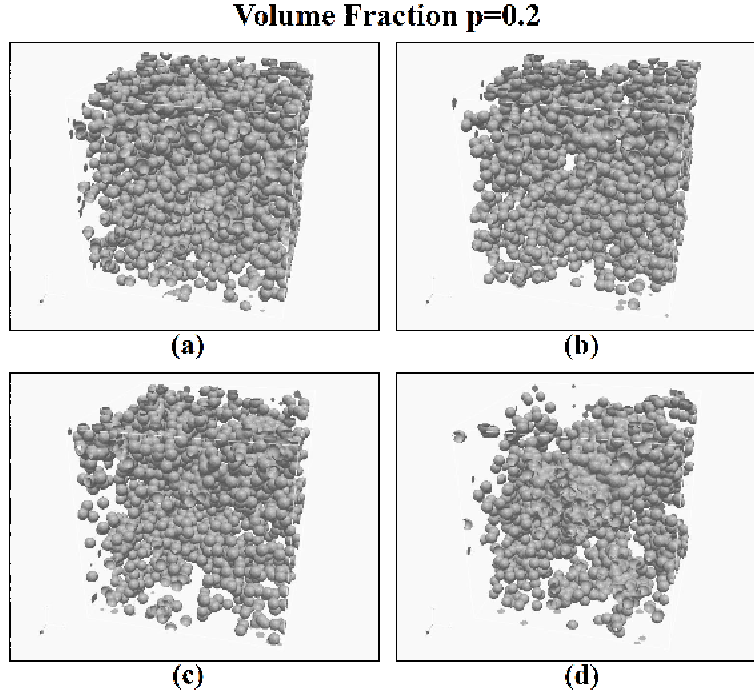


Fig. 2. The agglomeration parameters: Random particle systems with the agglomeration parameter $\gamma_{\text{agg}} = 0.0, 0.5, 0.8$ and 0.95 for (a), (b), (c) and (d) respectively.

In other words, if we take γ which is smaller than γ_{agg} , the added particle must be connected with the previous configuration \mathfrak{R}_n . Thus, γ_{agg} stands for the agglomeration of the particle system.

By monitoring the total volume fraction which is a function of \mathfrak{R}_n and is denoted by $\text{vol}(\mathfrak{R}_n)$, we continue to put the particles as long as $\text{vol}(\mathfrak{R}_n) \leq p$ for a given volume fraction p . We find the step $n(p)$ such that $\text{vol}(\mathfrak{R}_{n(p)-1}) \leq p$ and $\text{vol}(\mathfrak{R}_{n(p)}) > p$. Since the difference between $\text{vol}(\mathfrak{R}_{n(p)-1})$ and $\text{vol}(\mathfrak{R}_{n(p)})$ is at most 1.5×10^{-5} for the employed parameters. Thus we regard $\text{vol}(\mathfrak{R}_{n(p)})$ as the volume fraction p itself hereafter under this accuracy.

As illustrated in Figure 2, the uniform random configuration is realized as the case $\gamma_{\text{agg}} = 0$, and the agglomeration configurations are given with our agglomeration parameter $\gamma_{\text{agg}} > 0$. We regard ACPM of the case $\gamma_{\text{agg}} = 0$ as the ordinary CPM for balls with the same radius^{11,17} and thus we simply call it CPM hereafter.

Since we use the pseudo-randomness to simulate the random configuration $\mathfrak{R}_{n(p)}$ for the given p and γ_{agg} , the configuration $\mathfrak{R}_{n(p)}$ also depends upon the seed i_s of

6 *S. Matsutani, Y. Shimosako, Y. Wang*

the pseudo-random which we choose. We let it be denoted by $\mathfrak{R}_{\gamma_{\text{agg}},p,i_s}$. For the same seed i_s of the pseudo-random, a configuration $\mathfrak{R}_{\gamma_{\text{agg}},p,i_s}$ of a volume fraction p naturally contains a configuration $\mathfrak{R}_{\gamma_{\text{agg}},p',i_s}$ for $p' < p$ due to our algorithm. Hence the elements in the set of the configurations $\{\mathfrak{R}_{\gamma_{\text{agg}},p,i_s} \mid p \in [0, 1]\}$ with the same seed i_s are relevant. As shown later, the conductivity curve (1) over $\{\mathfrak{R}_{\gamma_{\text{agg}},p,i_s} \mid p \in [0, 1]\}$ is obtained as a smooth curve even for the non-vanishing γ_{agg} .

In order to illustrate this algorithm, we will show two dimensional case. The same as the three-dimensional case, we have two dimensional agglomeration configurations which are given in Figure 3. Figure 4 exhibits the transmission electron micrograph (TEM) of the real agglomerated particles in Refs. 8 and 20. Ref. 8 is of the composite of polyacrylonitrile with acetylene black particles, and Ref. 20 shows the epoxy nanocomposites with silicate oxide particles. These configurations in Figure 3 might simulate some agglomeration states in Figure 4. Even though it is difficult to visualize the three dimensional cases well, it is expected that our algorithm generates the similar agglomerate configurations.

2.2. Computation of the conductivity in ACPMs

To apply FDM² to the computation of the conductivity in ACPM, we use a $N_x \times N_y \times N_z$ lattice denoted by \mathcal{L} to represent the box-region \mathcal{B} by the integers N_x , N_y and N_z . In this article, we mainly assume that $N_x = N_y = N_z = 216$ and the radius of the particle $\rho = 1$ corresponds to six meshes. It means that the ratio between the volumes of \mathcal{B} and a particle is about 6.7×10^4 and the size of $\mathcal{B} = [0, L]^3$ is given as $L \approx 36$.

Further we set the conductivity distribution $\sigma(x, y, z)$ which consists of the conductive particles and insulator as background in the box-region \mathcal{B} as in Figure 2. We put the conductivity density $\sigma_{\text{mat}} = 1$ inside of each $\mathfrak{R}_{\gamma_{\text{agg}},p,i_s}$. As the insulator, we set the infinitesimal conductivity $\sigma_{\text{inf}} = 10^{-4}$ in its background. In other words, we handle binary materials with largely different local conductivities σ_{mat} and σ_{inf} .

In order to compute the total conductivity, we set the voltage $\phi = \phi_0 = 1$ and $\phi = 0$ on the upper and the lower faces, *i.e.*, $[0, x_0] \times [0, y_0] \times \{z_0\}$ and $[0, x_0] \times [0, y_0] \times \{0\}$ respectively as the boundary condition corresponding to the electrodes. As the side boundary condition, we used the natural boundary for each yz -face and each xz -face. In other words, at the side boundaries, we imposed that current normal to each face vanished.

Following our algorithm of FDM as mentioned in detail in Ref. 1, we numerically solved the generalized Laplace equations over the region,

$$\nabla \cdot \sigma \nabla \phi = 0, \quad (2)$$

for the conductivity distribution $\sigma(x, y, z)$ for each $\mathfrak{R}_{\gamma_{\text{agg}},p,i_s}$ to obtain the potential distribution $\phi(x, y, z)$. By numerically solving (2), we obtained the total conductivity σ_{total} of the system after we integrated the current $\sigma \nabla \phi$ over a xy -plane. Since σ_{total} is determined for each $\mathfrak{R}_{\gamma_{\text{agg}},p,i_s}$, σ_{total} is a function of the volume fraction

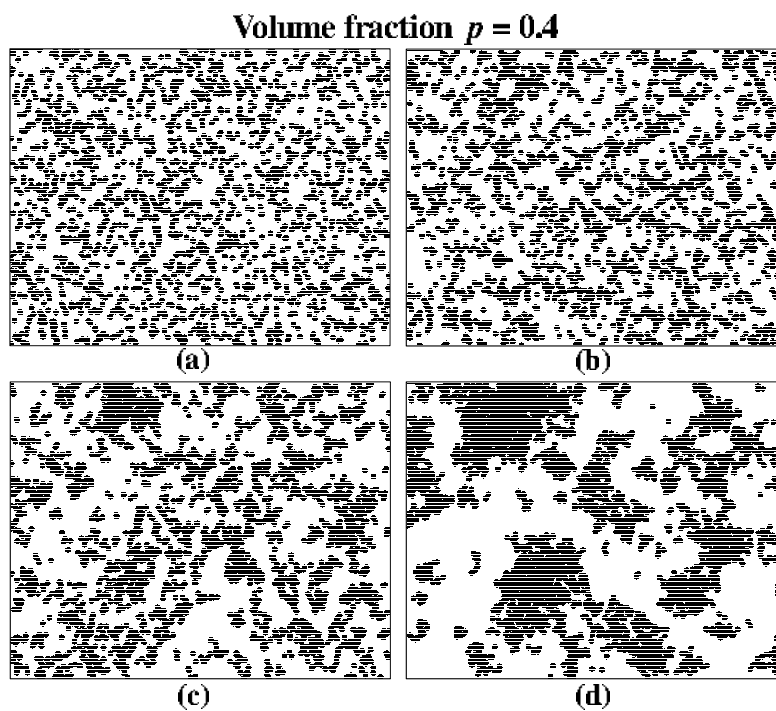


Fig. 3. The agglomeration parameters: Random particle system with the agglomeration parameter $\gamma_{\text{agg}} = 0.0, 0.5, 0.8$ and 0.95 for (a), (b), (c) and (d) respectively.

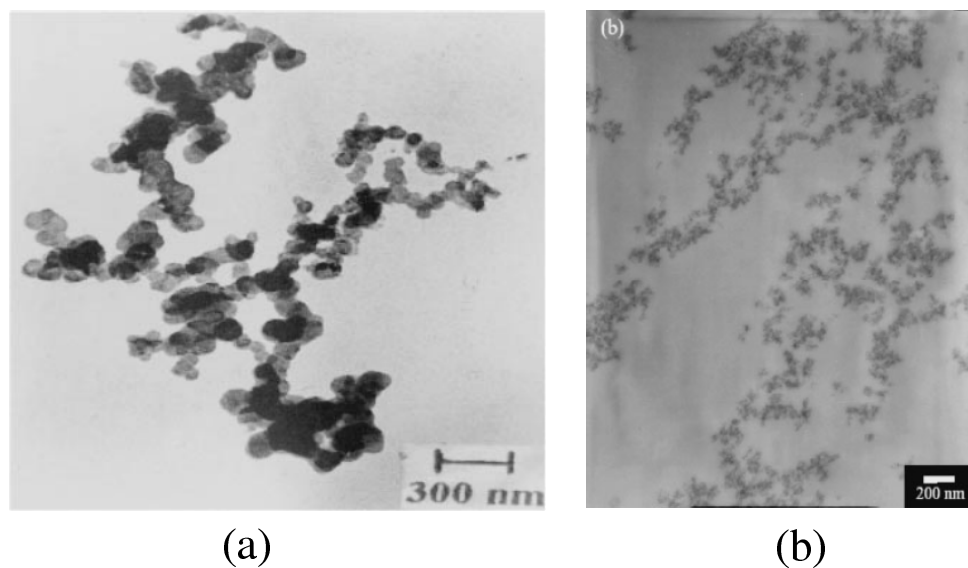


Fig. 4. TEM micrograms of (a) polyacrylonitrile nanocomposite of acetylene black particles in Ref.9 and (b) epoxy nanocomposites containing silicate oxide particles. in Ref.21

8 *S. Matsutani, Y. Shimosako, Y. Wang*

p , γ_{agg} and the seed i_s of the pseudo-random. We denote it by $\sigma_{\text{total}}(p, \gamma_{\text{agg}}, i_s)$ explicitly or simply $\sigma_{\text{total}}(p)$.

As mentioned in Introduction, the conductivity curve $\sigma_{\text{total}}(p)$ ($p \in [0, 1]$) is expressed by

$$\sigma_{\text{total}}(p) = \begin{cases} \frac{(p-p_c)^t}{(1.0-p_c)^t}, & \text{for } p \in [p_c, 1], \\ 0 & \text{otherwise,} \end{cases} \quad (3)$$

where the p_c is the threshold and t is the critical exponent, or merely exponent. Since the threshold p_c and the exponent t are determined by $\{\mathfrak{R}_{\gamma_{\text{agg}}, p, i_s} \mid p \in [0, 1]\}$, they are functions of the agglomeration parameter γ_{agg} and the random seed i_s . Thus we sometimes express them as $p_c(\gamma_{\text{agg}}, i_s)$ and $t(\gamma_{\text{agg}}, i_s)$.

We evaluated the exponent t and the threshold p_c as the fitting parameters so that each average of the square error from the curve is the smallest, by monitoring the square root of the average of the square error. The square root of the average of the square error is denoted by $\delta\sigma_{\text{total}} \equiv \delta\sigma_{\text{total}}(\gamma_{\text{agg}}, i_s)$.

3. Results

As mentioned above, for each seed i_s of the pseudo-random, a configuration $\mathfrak{R}_{\gamma_{\text{agg}}, p, i_s}$ to a volume fraction p naturally contains the configuration $\mathfrak{R}_{\gamma_{\text{agg}}, p', i_s}$ to $p' < p$ of the same seed i_s . Hence for a given seed i_s , the total conductivities σ_{total} between $\mathfrak{R}_{\gamma_{\text{agg}}, p, i_s}$ and $\mathfrak{R}_{\gamma_{\text{agg}}, p', i_s}$ are relevant. Thus we obtained the conductivity curve over $\{\mathfrak{R}_{\gamma_{\text{agg}}, p, i_s} \mid p \in [0, 1]\}$ as a smooth curve even with the vanishing γ_{agg} .

Figure 5 illustrates the conductivity curve for the seed $i_s = 1$. Figure 5 (b) shows that we handled the binary conductive materials. When $p = 0$, the total conductivity σ_{total} is equal to σ_{inf} which stands for the insulator and is negligible if we dealt with σ_{total} linearly as shown in Figure 5 (a). By using the least square error fitting method, we evaluated the threshold $p_c(\gamma_{\text{agg}}, i_s)$ and the exponent $t(\gamma_{\text{agg}}, i_s)$ from the curve. In the evaluation, we used the linear scale of σ_{total} or the curves in Figure 5 (a). Figure 6 shows the fitting errors $\delta\sigma_{\text{total}}$ v.s. the seed i_s ; $\delta\sigma_{\text{total}}$ is the average of the squares of the deviations from the curve (3) over the fitting points for each γ_{agg} and i_s ; the fitting points are 0.0, 0.1, 0.15, 0.2, 0.25, 0.3, 0.4, 0.5, 0.7, 0.9, and 1.0. We computed thirty curves for each case, $\gamma_{\text{agg}} = 0.0, 0.5, 0.8$ and 0.95 . The deviations $\delta\sigma_{\text{total}}$ are not large even for non-vanishing γ_{agg} compared with $\sigma_{\text{mat}} = 1$. The distribution of $\delta\sigma_{\text{total}}$ shows that for larger γ_{agg} , the values are large, and its maximum is $\delta\sigma_{\text{total}, \text{max}} \leq 0.026$ for $\gamma_{\text{agg}} = 0.95$, but the average $\overline{\delta\sigma_{\text{total}}}$ is less than 0.012; the values of $(\gamma_{\text{agg}}, \overline{\delta\sigma_{\text{total}}})$ are given as (0.0, 0.005), (0.5, 0.008), (0.8, 0.012) and (0.95, 0.012).

It means that the thresholds p_c and the exponents t represent the conductivity curves well in our computations. In fact since we have

$$\frac{\partial\sigma_{\text{total}}(p)}{\partial p_c} = -\sigma_{\text{total}}(p) \frac{1-p}{(1-p_c)(p-p_c)} t, \quad \frac{\partial\sigma_{\text{total}}(p)}{\partial t} = \sigma_{\text{total}}(p) \log \frac{p-p_c}{1-p_c},$$

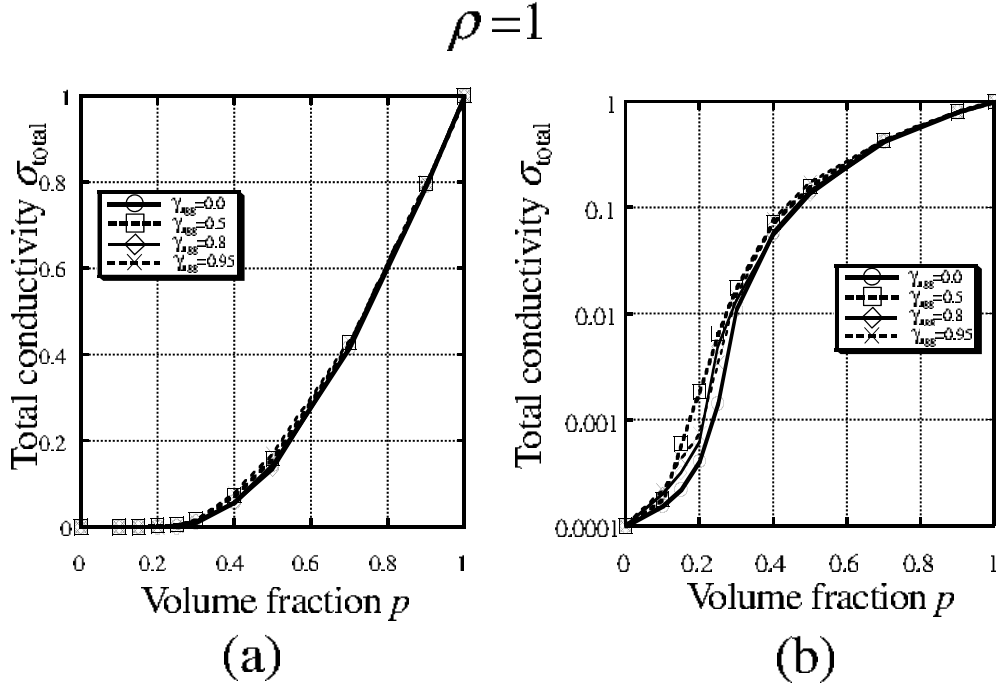


Fig. 5. The conductivity curves for agglomeration parameters of the random seed $i_s = 1$ γ_{agg}

the accuracies $\delta_{\sigma} p$ and $\delta_{\sigma} t$ of p_c and t , could be estimated using $\delta \sigma_{\text{total}}$;

$$\delta_{\sigma} p = \left| \left(\frac{\partial \sigma_{\text{total}}}{\partial p_c} \right)^{-1} \right| \overline{\delta \sigma_{\text{total}}}, \quad \delta_{\sigma} t = \left| \left(\frac{\partial \sigma_{\text{total}}}{\partial t} \right)^{-1} \right| \overline{\delta \sigma_{\text{total}}}.$$

For example, around $p \approx 0.5$ ($\sigma_{\text{total}} \approx 0.2$), they are evaluated as $\delta_{\sigma} p \approx \overline{\delta \sigma_{\text{total}}} \approx 0.01$ and $\delta_{\sigma} t \approx 5 \overline{\delta \sigma_{\text{total}}} \approx 0.06$ by setting $p_c \sim 0.3$, $t \sim 1.5$ as shown later.

As the case $\gamma_{\text{agg}} = 0$, our computational results are that $p_c = 0.305 \pm 0.007$ and $t = 1.504 \pm 0.002$, which agree with $p_c = 0.295 \pm 0.006$ in Ref. 14. and $t = 1.6 \pm 0.1$ in Refs. 21 and 22. However they are slightly different, $\delta p_c \approx 0.01$ and $\delta t \approx 0.08$, from the recent results in $p_c = 0.296 \pm 0.013^1$ and $p_c = 0.2854$ of Ref. 19 and $t = 1.58 \pm 0.06^1$ because in Refs. 1 and 19, these were corrected so that they exhibit the values over the region with the infinite L by an extrapolation method. Though the differences are also interpreted by the size effect which we will discuss the following section, the differences are not large and thus we go on to investigate the computational results without any further corrections in this article. In other words, since $\delta p_c \sim \delta_{\sigma} p_c$ and $\delta t > \delta_{\sigma} t$, we will investigate the system in these accuracies $\delta p_c \approx 0.01$ and $\delta t \approx 0.08$.

The dependences of exponents and thresholds upon the agglomeration parameter γ_{agg} are illustrated in Figure 7 and Table 1. Figure 7 shows that the agglomeration

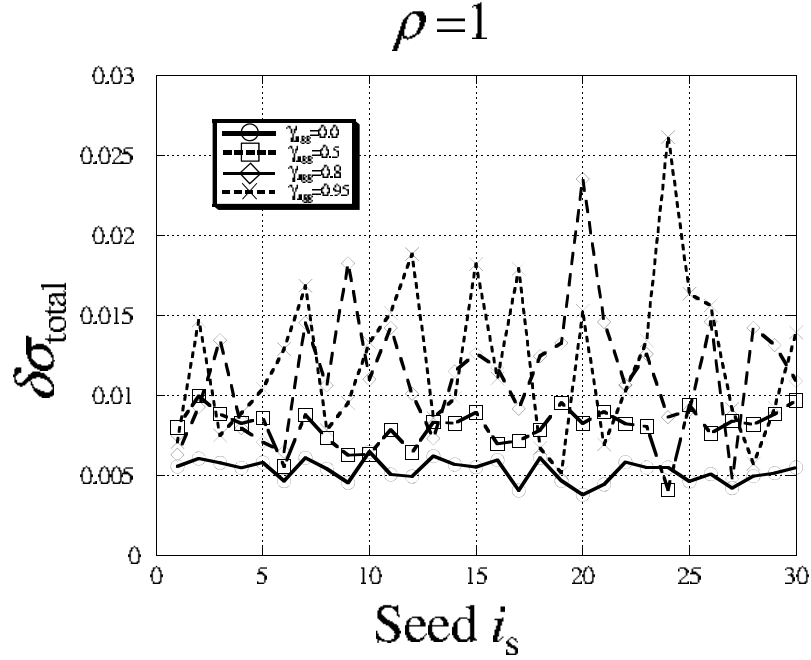


Fig. 6. The fitting errors $\delta\sigma_{\text{total}}$ vs the random seed i_s . γ_{agg}

parameter γ_{agg} has large effects on the conductivity over ACPM beyond the accuracies $\delta p_c \approx 0.01$ and $\delta t \approx 0.08$. When γ_{agg} deviates farther from 0, the dependence of the threshold and exponent on the seed becomes larger. It means that the fluctuation coming from the randomness is enhanced by the agglomeration parameter γ_{agg} .

Furthermore the trend of the threshold becomes smaller and that of the exponent becomes larger depending upon the agglomeration parameter γ_{agg} . As shown in Table 1, the average of the thresholds p_c is smaller and the average of the exponent t is larger for larger γ_{agg} . Even though the difference among the exponents t shows the equivalent order to $\delta t \approx 0.08$, we regard that they show the trend certainly.

Table 1 The γ_{agg} dependence of the threshold and the exponent

γ_{agg}	Threshold			Exponent		
	Average	Maximum	Minimum	Average	Maximum	Minimum
0.0	0.305	0.310	0.298	1.504	1.505	1.502
0.5	0.297	0.309	0.283	1.508	1.515	1.503
0.8	0.284	0.316	0.193	1.539	1.871	1.503
0.95	0.251	0.336	0.047	1.619	2.204	1.504

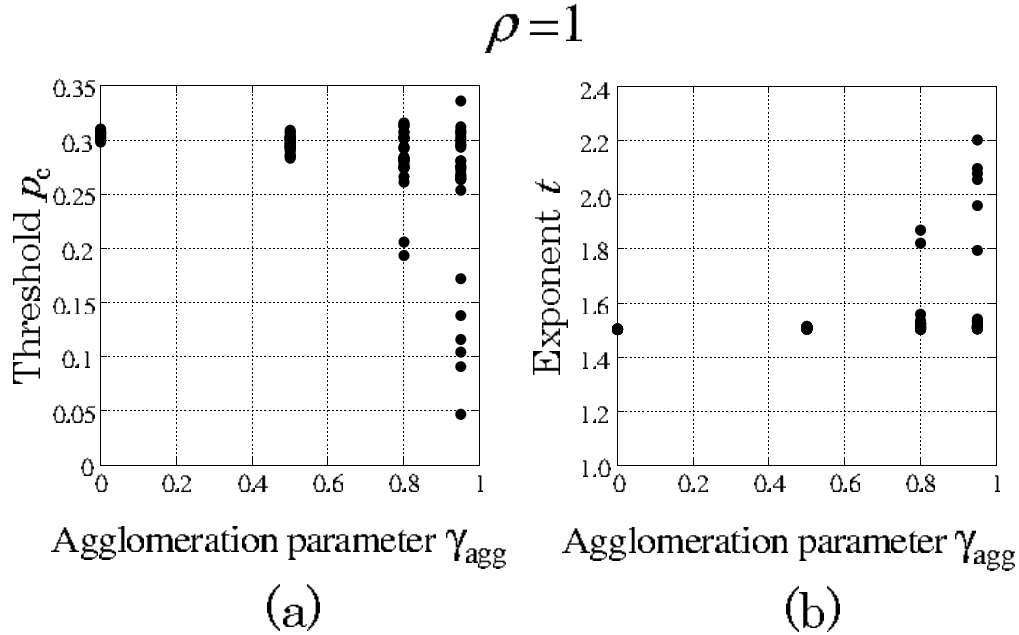


Fig. 7. The conductivity and critical exponents of three dimensional case:

4. Discussion on the agglomeration effects

We now consider the reason why the agglomeration has the effects on the conductivity in our ACPM. Since we have dealt with the percolation phenomena on a finite region \mathcal{B} , and the agglomeration must have an influence on the size of the percolation cluster, we first review the size effect on the conductivity following Ref. 3 and simply consider it in CPM numerically.

4.1. The size effect on conductivity in CPM

It is well-known that the conductivity has a dependence on the size of region as in Chapter 5.1 in Ref. 11, we consider the conductivity in CPM or the case $\gamma_{\text{agg}} = 0$ here.

As we wrote in Introduction, we naturally have the characteristics length induced from the size of the particles or the radius of the particle ρ . Further by letting $\xi = \xi(p, \gamma_{\text{agg}})$ be the correlation length which represents the percolation phenomenon, we should compare the size of region L , the correlation length ξ and the radius ρ .

According to Chapter 5.1 in Ref. 11, the total conductivity behaves like

$$\sigma_{\text{total}}(p, \gamma_{\text{agg}}) \propto \begin{cases} \xi^{-\mu}, & \text{for } L \gg \xi, \\ L^{-\mu}, & \text{for } L \ll \xi, \end{cases} \quad (4)$$

where μ is the non-negative parameter (73a) in Ref. 11. Since it is known that ξ diverges at the critical point p_c and in every numerical estimation we handle only a finite region, the formula (4) means that every numerical estimation gives higher conductivity in the vicinity of the point p_c than that of infinite region. The percolation theory is basically concerned with conductivity curve in the infinite region.

However we concern ourselves about the size effect of the real materials. Instead of the corrections of data so that using the results, we estimate ones in the infinite region as in Ref. 1, we will consider the size effect by changing ρ in this subsection.

Since ξ must converge to zero at $p = 1$, on the region ($1 > p \gg p_c$), the variation of ρ affects the conductivity weakly. However around p_c , $\sigma_{\text{total}}(p, \gamma_{\text{agg}} = 0, i_s)$ is influenced with the size L drastically since ξ and L are scaled by ρ .

The characteristic length is $\rho = 1$ in our CPMs ($\gamma_{\text{agg}} = 0$) and thus the length L of the system \mathcal{B} should be measured by the radius ρ , which is $L \approx 36$ for $\rho = 1$. When we fix \mathcal{B} , for larger ρ , the effective L in (4) is smaller. It is expected that the total conductivity $\sigma_{\text{total}}(p, \gamma_{\text{agg}} = 0, i_s)$ strongly depends on the configuration $\mathfrak{R}_{\gamma_{\text{agg}}=0, p, i_s}$ because we don't have sufficiently many particles and its statistical average does not work well. It means that the dependences of the threshold $p_c(\gamma_{\text{agg}} = 0, i_s)$ and the exponent $t(\gamma_{\text{agg}} = 0, i_s)$ on the seed i_s are larger.

Furthermore, around p_c , the size effect is larger and from (4), the total conductivity σ_{total} does not vanish even around p_c . It means that the estimation of p_c should be smaller than that in the infinite one.

We computed the threshold p_c and exponent t for the larger size ρ of the radius by fixing the size of \mathcal{B} . Figure 8 shows these behaviors for different system sizes. From the numerical viewpoint, we performed the similar computations of $\gamma_{\text{agg}} = 0$ for smaller $N_x = N_y = N_z$ by fixing the mesh of ρ . It corresponds to the variation of the radius ρ of the particles for fixing \mathcal{B} relatively.

Figure 8 gives the dependence of the exponents and the threshold on the size of particles for the same \mathcal{B} . As mentioned above, for a (relatively) larger size of ρ , the fluctuations of the threshold p_c and the exponent t are larger, and the trend of p_c is smaller as mentioned above. The tendency is very similar to the Figure 7 if the agglomeration parameter γ_{agg} reads the size of ρ appropriately.

Even for the case which the p_c is smaller than that of $\rho = 1$, it is expected that around p_c the total conductivity σ_{total} is very small and increases weakly. It implies that t is larger in the conductivity curve (3). In fact Figure 9 (b) exhibits the correlation between the thresholds and the exponents in both the agglomeration effects and size effects. The smaller p_c has, the larger the exponent t is. The behaviors for both the agglomeration effect and the size effect are essentially the same.

4.2. *The agglomeration effect on conductivity in ACPM*

We now consider one of the effects of the agglomeration on the conductivity in our ACPM with $\rho = 1$ as the size effect as mentioned in the previous subsection.

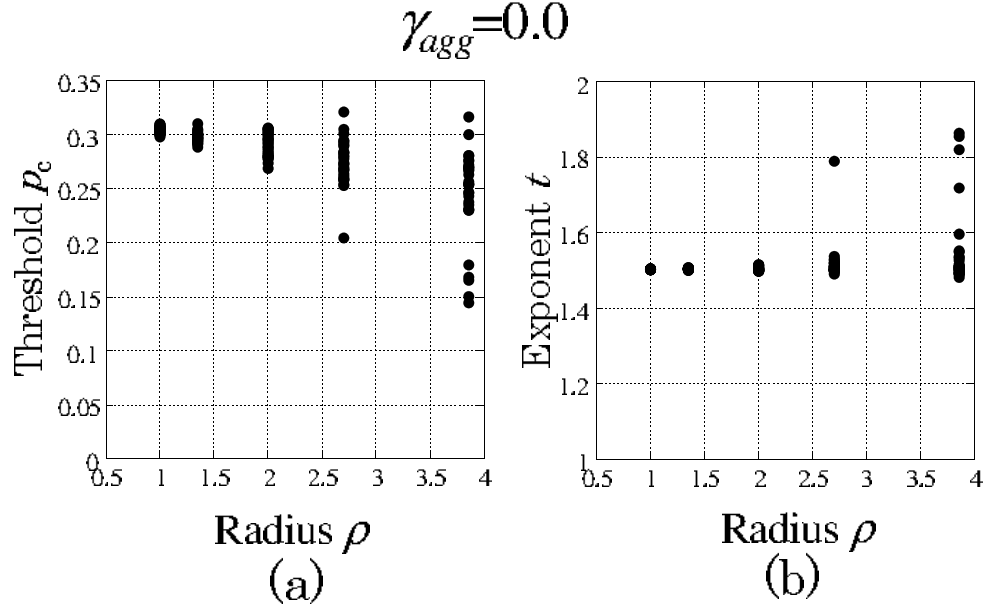


Fig. 8. Critical exponents and thresholds vs radius of particles in the same \mathcal{B} . γ_{agg}

When the agglomeration parameter γ_{agg} becomes larger, it is expected that the size of the percolation cluster becomes larger than one of the uniform random or the case ($\gamma_{agg} = 0$). The size of the percolation cluster is associated with the correlation length $\xi(p, \gamma_{agg})$ in (4).

In order to evaluate the effect of the size, we consider a histogram of the size of the percolation clusters, or the connected particles. Figure 10 shows frequency of the effective radius ρ_{class} of the volume of the percolation cluster at $p = 0.1$ which is smaller than any thresholds p_c . Here the effective radius ρ_{class} is defined such that $4\pi\rho_{class}^3/3$ is equal to its volume. Figure 10 shows that for larger γ_{agg} , the size of the cluster is larger.

Figure 10 shows the fact that the histogram has two peaks; the first peak at $\rho_{class} = 1$ as the size of isolated particle, and the second peak around $\rho_{class} = \sqrt[3]{2} \approx 1.26$ as the size of two particles. The probability of two slightly connected particles is larger than ones over $\rho_{class} \in (1, \sqrt[3]{2})$ because of radial measure of $\rho_{class}^2 d\rho_{class}$ for the radius ρ_{class} from the center of a particle. The percolation is determined by the largest cluster size but it should be statistically treated. We consider the right hand side of the second peak of the histograms. We fit the shape of the histogram over $\rho_{class} \in [1.3, 8]$ by $h(\rho_{class}) = A \exp(-(\rho_{class} - 1)/\rho_{class}^0)$ well using the least mean square error method, where A and ρ_{class}^0 are fitting parameters. Then ρ_{class}^0 is given by the

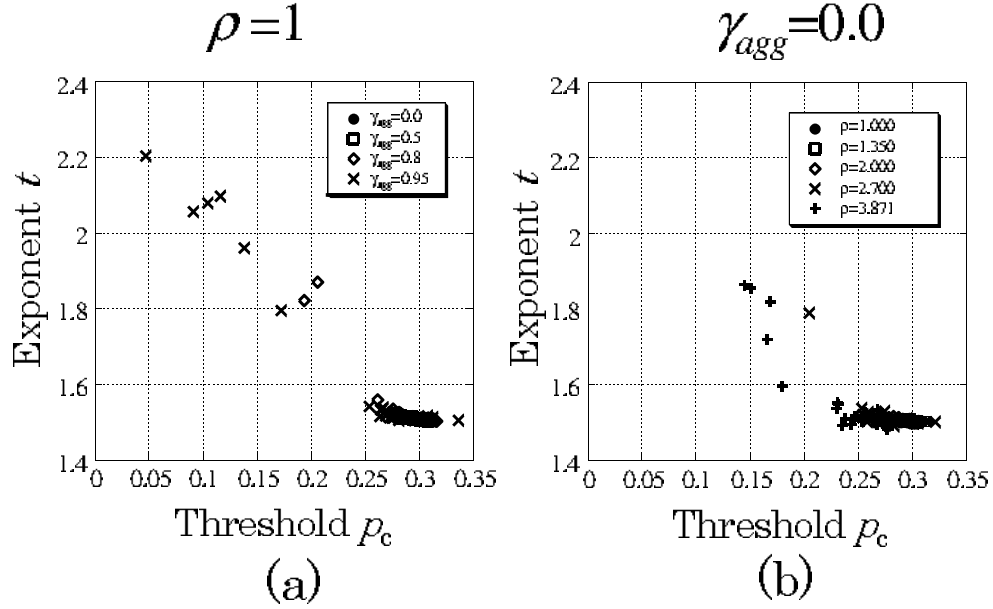


Fig. 9. Critical exponents vs thresholds for various γ_{agg} with (a) $\rho = 1$, and for various ρ with (b) $\gamma_{agg} = 0.0$.

following table. Here δh is the square root of the average of the least mean square error.

Table 2 The ρ_{class} dependence on the agglomeration parameter γ_{agg}

γ_{agg}	0	0.5	0.8	0.95
ρ_{class}^0	0.241	0.310	0.331	0.349
δh	0.002	0.006	0.006	0.011

Table 2 shows that the agglomeration parameter γ_{agg} increases the size of the clusters at $p = 0.1$. Though it is difficult to evaluate the difference of the size of clusters ρ_{class}^0 at $p \geq p_c$, it is expected that it plays similar roles even for every $p \in [0, 1]$.

It means that the agglomeration parameter γ_{agg} makes the size of the percolation clusters larger and effective size L in (4) relatively smaller. For the agglomeration parameter γ_{agg} deviated from 0, \mathcal{B} corresponds to a relatively smaller region than the uniform random case ($\gamma_{agg} = 0$). It means that the threshold becomes smaller in our evaluation due to the finite size effect, and the dependences of the threshold and

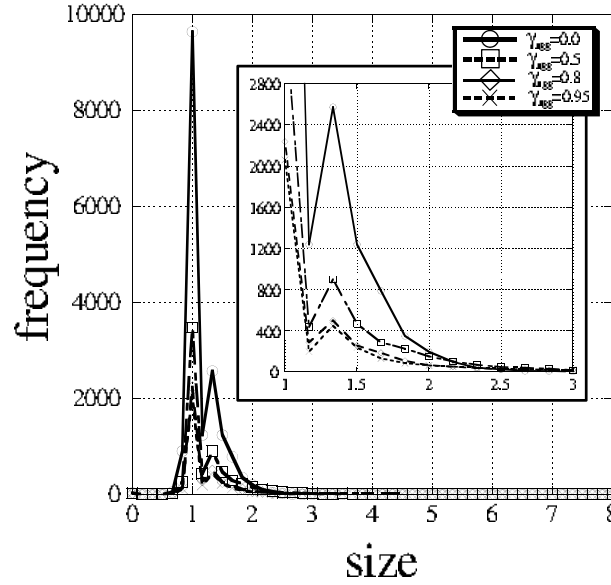


Fig. 10. The histogram of size of percolation cluster for each agglomeration parameter γ_{agg} .

the exponent upon the seed of the pseudo-random are larger or these fluctuations are larger. It is expected that the trend of the threshold p_c to $\gamma_{\text{agg}} > 0$ is smaller than p_c at the case $\gamma_{\text{agg}} = 0$ even though there is a large fluctuation of p_c . The results in Figure 7 show such properties. As mentioned in §4.1, the smaller p_c is related to the larger t . Figure 9(a) and Figure 7 show that γ_{agg} enhances the exponent t in the conductivity curve (3).

Thus we conclude that the agglomeration has the effect on the characteristic size of the percolation system and it makes the relative size of the total system small so that the fluctuation due to the randomness becomes larger.

Conversely it implies that the agglomeration would not have the effect on the universality class of the conductivity curve (3) though we numerically show that the shape of particles influences the universality class in the previous article.¹ In other words, for larger agglomeration parameter γ_{agg} , if we properly deal with a system \mathcal{B} with sufficiently large size, the conductivity curve might be the same as the uniform random case ($\gamma_{\text{agg}} = 0$).

Figure 11 exhibits the dependence of conductivity curves on the size of the system for the $\gamma_{\text{agg}} = 0.5$ case. In the computation of Figure 11, we used larger $N = N_x = N_y = N_z$ analyzed regions as $N = 272$ and $N = 344$. The relative

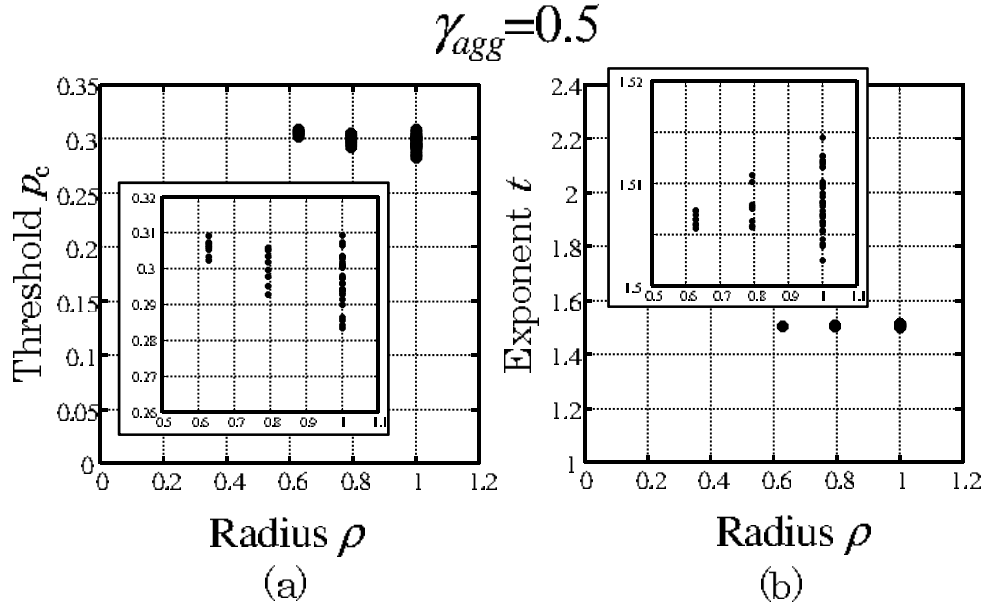


Fig. 11. The dependence of the thresholds and exponents on the size of the system for ACPM with $\gamma_{agg} = 0.5$

particle sizes (the radii) are $\rho = 0.79$ and $\rho = 0.63$. Since these computations are harder than $N = 216$, we computed only eight curves for these additional cases respectively as shown in Figure 11 and Table 3.

Table 3 The ρ dependence of the threshold and the exponent for the case $\gamma_{agg} = 0.5$

ρ	Threshold			Exponent		
	Average	Maximum	Minimum	Average	Maximum	Minimum
1.00 [†]	0.297	0.309	0.283	1.508	1.515	1.503
0.79*	0.300	0.306	0.293	1.508	1.511	1.506
0.63*	0.306	0.309	0.302	1.507	1.507	1.506

*: eight curves. [†] thirty curves.

Though we might need to discuss more about their accuracy, they may show that the asymptotic behavior of the thresholds p_c and the exponents t recover those of the case $\gamma_{agg} = 0.0$. It implies that the agglomeration, at least in the case of our algorithm of agglomeration, might have no effect on the universality class.

5. Summary

By employing the simple algorithm to simulate an agglomerated configuration of particles in CPM or ACPM, which is controlled by the agglomeration parameter $\gamma_{\text{agg}} \in [0, 1]$, we numerically show how the thresholds p_c and the exponent t of the conductivity curve (3) depend upon the agglomerations as shown in Figure 7. In other words, the fluctuation due to the randomness is larger when γ_{agg} is deviated from 0 farther. Further the trend of the thresholds becomes smaller and that of the exponents becomes larger for the larger agglomeration parameter γ_{agg} .

From §4, we conclude that the origin of these effects could be interpreted as the size effect because the agglomeration makes the percolation cluster larger and effective size of the particles larger. Furthermore it is conjectured conversely that the agglomeration parameter might have no effects on the universality class of the threshold and the exponents if we handle the analyzed region with the sufficiently large size.

Due to the development of the technology, smaller sizes of devices and conductive nanoparticles are concerned. Then in the conductivity in the composite materials of the conductive nanoparticles, the size effect and the agglomeration effect have crucial roles. We believe that our results shed a new light on the applications of the percolation theory to such a real material system.

References

1. S. Matsutani, Y. Shimosako, and Y. Wang, *Int. J. Mod. Phys. C* **21** (2010) 709-729.
2. R. J. LeVeque, *Finite Difference Methods for Ordinary and Partial Differential Equations: Steady-State and Time-Dependent Problems (Classics in Applied Mathematics)*, (Soc. for Industrial & Applied, 1955 republished in 2007).
3. M. H. Al-Saleh and U. Sundararaj, *Eur. Polymer J.* **44** (2008) 1931-1939
4. Y. Konishi and M. Cakmak, *Polymer* **47** (2006) 5371-5391.
5. H-H. Leea, K-S. Choua, and Z-W. Shih, *Int. J. of Adhesion & Adhesives* **25** (2005) 437-441.
6. Z. Ranjbar and S. Rastegar, *Colloids and Surfaces A : Physicochem. Eng. Aspects* **290** (2006) 186-193.
7. H.P. Wu, X.J. Wu, M.Y. Ge, G.Q. Zhang, Y.W. Wang and J.Z. Jiang , *Composites Sci. and Tech.* **67** (2007) 1116-1120.
8. A. Maity and M. Biswas, *Polymer J.*, **36** (2004). 812-816.
9. I. Tail, G. I. Tardos, and M. I. Khan, *Powder Tech.* **110** (2000) 59-75
10. P. Kosinski, and A. Hoffmann, *Chem. Eng. Sci.* **65** (2010) 3231-3239
11. D. Stauffer and A. Aharony, *Introduction to percolation theory, revised second ed.*, (CRC Press, Boca Raton, 1991).
12. G. E. Pike and C. H. Seager, *Phys. Rev. B* **10** (1973) 1421-1434.
13. G. E. Pike and C. H. Seager, *Phys. Rev. B* **10** (1973) 1435-1446.
14. M. B. Isichenko, *Rev. Mod. Phys.* **64** 961-1043.
15. P. M. Kogut and J. P. Straley, *J. Phys. C* **12** (1979) 2151-2159.
16. I. Balberg, *Phys. Rev. Lett* **59** (1987) 1305-1308.
17. R. Meester and R Roy, *Continuum Percolation, Cambridge Tracts in Mathematics 119*, (Cambridge, Cambridge, 1996).

18 *S. Matsutani, Y. Shimosako, Y. Wang*

18. G. Grimmett, *Percolation, second ed.*, (Springer, Berlin, 1999).
19. E. J. Garboczi, K. A. Snyder, J. F. Douglas and M. F. Thorpe, Phys. Rev. E **52** (1995) 819-828.
20. C-C. Chu, J-J. Lin, C-R. Shiu and C-C. Kwan, Polymer J., **37** (2005). 239-245.
21. A. B. Harris and S. Kirkpatrick, Phys. Rev. B **16** (1977) 542-576.
22. I. Webman, J. Jortner, and M. H. Cohen, Phys. Rev. B **16** (1977) 2593-2596.